Chemical Engineering Journal 155 (2009) 691–697

Contents lists available at ScienceDirect

Chemical Engineering Journal

journal homepage: www.elsevier.com/locate/cej

Atrazine degradation by *in situ* electrochemically generated ozone

Ysrael Marrero Vera, Roberto José de Carvalho*, Mauricio Leonardo Torem, Bruno Abreu Calfa

Department of Materials Engineering, Pontifical Catholic University of Rio de Janeiro, 22453-900, Rio de Janeiro, RJ, Brazil

ARTICLE INFO

Article history:
Received 16 April 2009
Received in revised form 28 August 2009
Accepted 1 September 2009

Keywords:
Groundwater
Remediation
PbO_2 electrode
Electrochemistry
Ozone
Atrazine

ABSTRACT

A study on the evaluation of the effectiveness of atrazine degradation by *in situ* electrochemically generated ozone was conducted. Ti/β-PbO_2 electrodes were used as anodes for the ozone production. The rate of ozone generation, the ozone saturation concentration and the atrazine degradation rate increased with increasing current density. The maximum rate was close to 40 mg h^{-1}, the dissolved ozone concentration was 1.6 mg L^{-1} for a current density of 1.5 kA m^{-2} and the electrochemical efficiency was around 6%. The degradation data followed a pseudo first-order kinetic. The values of the rate constants were 6.2×10^{-3}, 8.8×10^{-3}, and 1.21×10^{-2} min^{-1} for 0.5, 1.0, and 1.5 kA m^{-2}, respectively. The degradation took place by the combined oxidation with O_3 and •OH generated at the Ti/β-PbO_2 anode surface and by ozone decomposition. The rate was electrochemically controlled up to approximately 90% of degradation and by mass transfer thereafter. The degradation mechanism was comprised mainly by dealkylation followed by a slow dechlorination of the atrazine molecule. Continuous atrazine degradation tests were conducted in a column containing a porous medium with the purpose of determining whether the *in situ* electrochemical production of the oxidants •OH/O_3 is effective at reducing the atrazine concentration in the transported flux across the bed. The work demonstrates the potential applicability of the continuous system for *in situ* atrazine degradation in underground waters, and provides a basis for the future development of this technology.

1. Introduction

The intensive use of pesticides in agriculture and the high persistence of many of these chemicals have required a rigorous control of possible environmental contaminations, especially of drinking water sources as groundwater.

Atrazine (2-chlorine-4-ethyl-6-isopropyl-1,3,5-triazine) is a herbicide of extensive use in Brazilian agriculture mostly for corn, cotton, sorghum and sugar-cane. It is frequently detected in natural waters [1] and has been known to affect the reproduction of aquatic flora and fauna [2]. Fig. 1 shows the chemical structure for atrazine.

Electrochemical reactive permeable barriers (e-barriers) are a new technology to treat groundwater employing groups of electrodes as the active substratum of the barrier [3]. A potential difference is applied to the electrodes producing oxidation–reduction reactions on the electrodes surface. E-barriers can be used together with *in situ* chemical oxidation, that is, an oxidant is electrochemically produced in one of the electrodes that make up the barrier. The oxidant degrades the dissolved contaminants in a subsurface medium instead of at the electrode surface.

Systems where oxidants, as molecular ozone, hydroxyl radical or hydrogen peroxide are electrochemically generated to degrade different chemical products, as those found in textile effluents [4] and stored pesticides [5], have their effectiveness proven. However, the oxidation of pollutants by *in situ* electrochemically generated ozone with the electrochemical system making up an e-barrier to remediate aquifers has not yet been reported in the literature. Ozone is a powerful oxidant ($e^0 = 2.08$ V vs. Standard Hydrogen Electrode Potential) and its decomposition does not generate toxic by-products. It has been frequently used to degrade organic compounds present in soils and aquifers.

The objective of this study was to evaluate the effectiveness, at a laboratory scale, of an innovative technology for the *in situ* degradation of atrazine. This technology results from the combination of an *in situ* advanced oxidation process with an e-barrier, using electrochemically generated ozone as the oxidant agent. The work was divided in three parts: (1) ozone production in an electrochemical cell at different values of current density and the determination of the dissolved ozone concentration; (2) batch atrazine degradation in aqueous solution at different current densities; (3) continuous atrazine degradation in a horizontally mounted column packed with washed sand. The porous bed parameters (porosity and dispersivity) and the mean residence time of a KCl tracer in the

* Corresponding author at: Department of Materials Engineering, Pontifical Catholic University of Rio de Janeiro, 22453-900, Rio de Janeiro, RJ, Brazil.
Tel.: +55 21 3527 1562; fax: +55 21 3527 1236.
E-mail address: rjcar@puc-rio.br (R.J.d. Carvalho).

1385-8947/$ – see front matter © 2009 Elsevier B.V. All rights reserved.
doi:10.1016/j.cej.2009.09.001

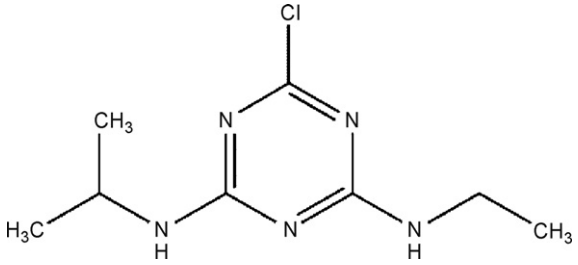

Fig. 1. Molecular structure of the atrazine herbicide.

column were determined. Atrazine degradation runs to evaluate the degradation efficacy as a function of the applied current were conducted.

2. Materials and methods

2.1. Electrochemical ozone production

Ti/β-PbO_2 electrodes were prepared by electrodeposition from a $Pb(NO_3)_2$ solution (0.2 mol L^{-1}; pH 2; 60 °C) on 0.5 mm thick titanium plates at constant anodic current density (0.2 kA m^{-2}; 20 min). An intermediate platinum layer was first electrodeposited on the plates from an aqueous solution of H_2PtCl_6 and $Pb(AcO)_2$ with concentrations 0.02 mol L^{-1} and 0.002 mol L^{-1}, respectively (0.3 kA m^{-2}; 5 min; 25 °C). For this purpose, the anode was a Ti/RuO_2 plate and the cathode was the titanium plate. The Ti/RuO_2 plate was supplied by De Nora Brasil. The β-PbO_2 coating was then electrodeposited on top of the platinum layer using the platinum coated titanium plate as anode and the Ti/RuO_2 plate as cathode.

The electrochemical ozone production for different current densities (0.5, 1.0 and 1.5 kA m^{-2}) was accomplished in a two-compartment cell (Fig. 2), one containing the β-PbO_2-coated titanium anode and the other the RuO_2-coated titanium cathode. The distance between anode and cathode was 4 cm and the fritted glass disk had a diameter of 4 cm. Each compartment had an approximate volume of 500 mL. The geometric area of the electrodes (anode and cathode) was 15 cm^2. A 0.1 M phosphate buffer solution (pH 7) was used. Nitrogen gas was passed through both compartments of the cell and the gas exiting the anode was bubbled through a 20 g L^{-1} KI solution. The iodine formed by the oxidation of iodide with ozone was determined by titration with sodium thiosulphate. A starch solution was used as indicator [6].

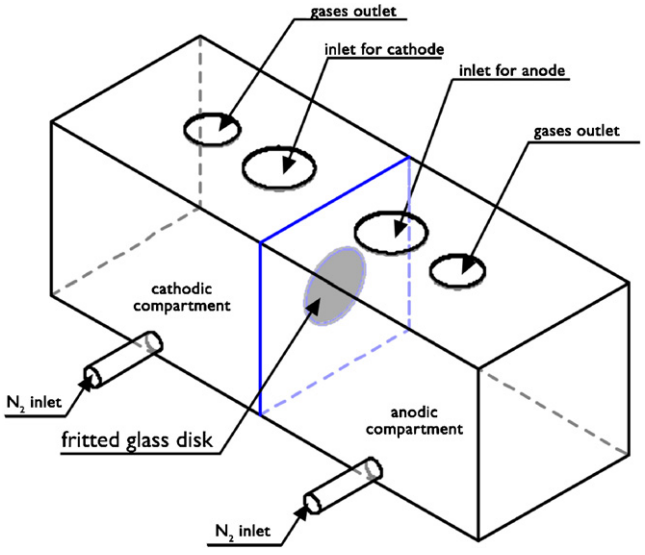

Fig. 2. Two-compartment cell used in the electrochemical ozone quantification experiments.

The current efficiency for ozone production was calculated using the follow expression (Eq. (1)).

$$\varepsilon = \frac{28950.C_{Na_2S_2O_3} \cdot V_{Na_2S_2O_3}}{i \cdot t} \quad (1)$$

where ε is the current efficiency for ozone production (%); $C_{Na_2S_2O_3}$ is the concentration of the sodium thiosulphate solution used in iodine titration (mol L^{-1}); $V_{Na_2S_2O_3}$ is the volume of thiosulphate solution consumed for iodine titration (mL), i is the current applied in the electrolysis experiment (A) and t the electrolysis time (s).

The determination of dissolved ozone was made in a one-compartment water-cooled cell. The electrodes and electrolytic solution were the same as above. The solution volume was 400 mL. Aliquots of 2 mL were removed from the cell and analyzed by the indigo method [7] to determine the dissolved ozone concentration.

2.2. Atrazine batch degradation experiments

The degradation of atrazine with *in situ* electrochemically generated ozone was carried through in a water-cooled glass cell with a capacity of 500 mL. 400 mL of a phosphate buffer solution containing 1 mg L^{-1} of atrazine was used in each experiment. The solution was agitated during the runs. Ozone was produced at the Ti/β-PbO_2 anode. The Ti/RuO_2 electrode was used as cathode. The degradation runs were conducted with current densities of 0.5, 1.0 and 1.5 kA m^{-2}. Solution samples were taken at some time intervals along the 6 h period of the runs. The concentrations of atrazine and of one of its degradation by-products were determined as a function of time. The liquid chromatographic system was a Varian ProStar 325 HPLC system equipped with a Varian Cary-100 double bean UV/vis spectrophotometer detector. A Varian Microsorb C18 separation column was used (length: 150 mm, internal diameter: 4.6 mm, particle diameter: 5 μm). The mobile phase for elution consisted of methanol, 65% (v/v) and water, 35% (v/v) water and the flow rate was 0.5 mL min^{-1}. The sample injection volume was 100 μL and the column temperature was 25 °C. A UV detector monitored the eluent; the detection wavelength was set at 222 nm. The wavelength was selected from the absorption spectra of a 1 mg L^{-1} atrazine solution and of a solution from an oxidation run containing the degradation by-products. The samples were not concentrated before the chemical analysis in the HPLC. The calibration curves for atrazine and the by-products desethylatrazine (DEA) and desisopropylatrazine (DIA) were obtained with certified analytical standards (Pestanal® 97.4% purity). The calibration curves were determined by measuring the area under the peaks for the concentration values of 0.1, 0.25, 0.5, 0.75 and 1 mg L^{-1}. The average of three area values for each standard concentration and the corresponding concentration were plotted and linearly fitted. The concentrations of the chemicals were determined from the equation of this straight line and from the areas computed in the chromatograms.

2.3. Column hydrodynamics

The column utilized in the oxidation experiments in a porous medium was made of acrylic and was cylindrical shaped. The total length of the column was 26 cm and its internal diameter was 4 cm (Fig. 3).

The packing material was washed sand with the particle size distribution presented in Table 1.

The packing of the column was carried out keeping it in a vertical position, introducing the sand and maintaining the water level in its interior slightly above the porous bed.

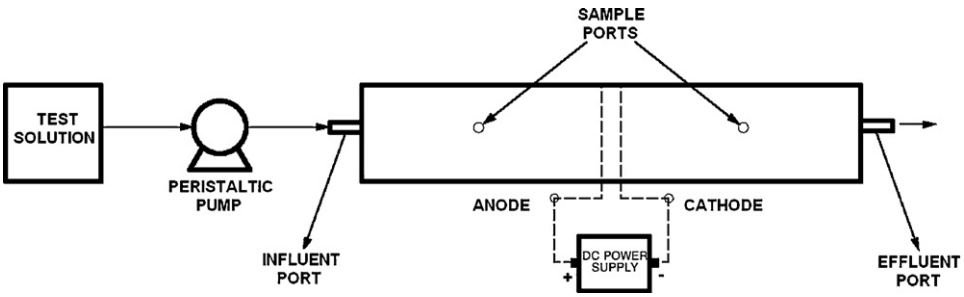

Fig. 3. Column reactor schematic and experimental setup.

A mass transfer experiment was performed to determine the hydrodynamic properties of the column. A KCl solution with a concentration of 1000 mg L^{-1} was applied as a tracer. The solution was pumped at a flow rate of 0.5 ml min^{-1} across the horizontally aligned column by a previously calibrated pulsating pump (Milan, model BP-200). The solution was periodically sampled and the concentration of KCl was determined by electric conductivity measurements. For this purpose, a concentration versus electric conductivity calibration curve was obtained from standard solutions with different concentrations of KCl. A one-dimensional advection–dispersion equation (Eq. (2)) was employed to adjust the experimental data and calculate the porous bed parameters [8].

$$C = \frac{C_0}{2}\left[\mathrm{erfc}\left(\frac{x - v_x t}{2\sqrt{Dt}}\right) + \exp\left(\frac{x v_x}{D}\right)\mathrm{erfc}\left(\frac{x + v_x t}{2\sqrt{Dt}}\right)\right] \quad (2)$$

where C is the concentration of KCl (mg L^{-1}), C_0 is the concentration of KCl at $x = 0$ (mg L^{-1}), x is the distance from the column entrance (cm), t is the elapsed time (min), D is the dispersion coefficient (cm^2 min), $v_x = q/(A \cdot n)$ is the average interstitial velocity of water (cm min^{-1}), q is the volumetric flow rate of injected solution (mL min^{-1}), A is the cross-section area of the column (cm^2) and n is the porosity of the packing. The dispersivity (cm) is equal to D/v_x.

Subsequently to obtaining the KCl concentration data as a function of time, the values of the average interstitial velocity of water, v_x, and of the dispersion coefficient, D, were determined by Eq. (2), for $x = 26$ cm (column length), with the aid of the Levenberg–Marquardt algorithm to perform nonlinear curve fitting. In possession of the values of v_x, A and q, the porosity, n, of the bed was calculated.

2.4. Continuous degradation of atrazine

Pesticide degradation experiments were conducted to evaluate the degradation efficacy as a function of the applied current in the column containing the porous bed.

The cathode consisted of a RuO_2-coated titanium expanded mesh and the anode of a β-PbO_2-coated titanium expanded mesh. The titanium expanded mesh was supplied by De Nora Brazil. The β-PbO_2 coating was electrodeposited on the titanium expanded mesh. The anode was mounted at 12.7 cm and the cathode at 13.3 cm from the column entrance. The inter-electrode space was filled with a layer of 6 mm glass beads. The 15 cm^2 electrodes were placed perpendicularly to the flux, thus, occupying the whole cross-section of the column.

The anode was the first electrode to come into contact with the solution flowing through the porous bed. Downstream to the electrodes there was 3 mm orifice for taking off the gaseous products of water electrolysis. During the experiments, a 0.1 M phosphate buffer solution (pH 7) containing 1.0 mg L^{-1} of atrazine was pumped at rate 0.5 mL min^{-1}. The degradation experiments lasted 8 h. Every 1 h, 1.0 mL of solution was sampled through rubber hoses located 6.5 cm upstream and downstream from the center of the column. Two runs were carried out, one at 0.4 A, and the other at 0.6 A. A third run was performed with no current imposed.

Table 1
Particle size distribution of the sand used as bed packing material.

Diameter, d (mm)	wt. %
$d > 0.59$	50.1
$0.21 < d < 0.59$	40.4
$0.062 < d < 0.21$	9.0
$d < 0.062$	0.5

3. Results and discussion

3.1. Ozone generation

The use of electrode materials having a high overpotential for the oxygen evolution reaction (e.g. β-PbO_2) combined with a supported electrolyte containing fluoro-compounds and low temperature to obtain the best efficiency for electrochemical ozone production is reported in the literature [9]. On the other hand, even under drastic conditions of current density and electrolyte acidity the β-PbO_2 can be considered an inert electrode material [10]. The adherence of the β-PbO_2 coating was good and X-ray diffraction analysis confirmed that the deposit contained only the α- and β-PbO_2 with the β phase prevailing.

The ozone generation rates after 15 min of experiment, the rates per geometric area of the electrode and the efficiencies of ozone production for different values of current density are shown in Table 2.

Gaseous ozone concentration was determined when a pH 7 buffer solution was used. At pH 7, the ozone decomposition rate was relatively high. The total ozone generated was the sum of the dissolved ozone and the decomposed ozone. The stripped ozone may not be the total ozone electrochemically produced.

These results show that both the ozone generation rate and the rate per geometric area of the electrode increased with increasing current density. It was also observed that the efficiency of ozone production depended on the applied current density. The efficiency value for 0.5 kA m^{-2} is significantly lower than the values for 1.0 and 1.5 kA m^{-2}. The values for 1.0 and 1.5 kA m^{-2} are in agree-

Table 2
Results of the ozone generation experiments.

Current density (kA m^{-2})	O_3 generation rate (mg h^{-1})	O_3 generation rate per electrode area (mg h^{-1} m^{-2})	Efficiency (%)
0.5	4.4 ± 1.0	29 ± 7	1.959 ± 0.005
1.0	19.5 ± 2.3	130 ± 20	6.69 ± 0.04
1.5	39.1 ± 1.0	261 ± 7	5.826 ± 0.002

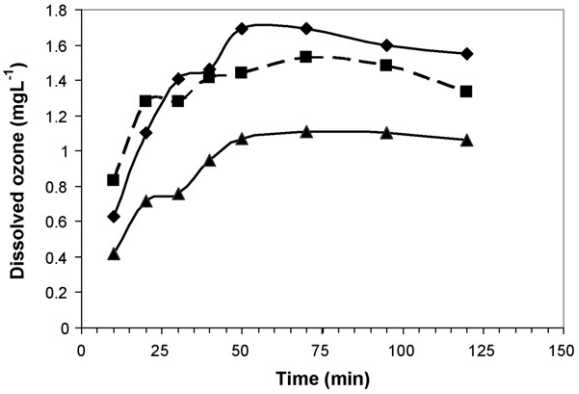

Fig. 4. Effect of current density on dissolved ozone concentration (▲) 0.5 kA m^{-2}; (■) 1.0 kA m^{-2} (♦) 1.5 kA m^{-2}.

ment with the efficiency of 5% observed by Graves et al. [11] for current densities ranging from 1.0 to 4.0 kA m^{-2} at room temperature, PbO_2-coated titanium electrodes and electrolytes consisting of oxianions (SO_4^{2-}, PO_4^{3-}, ClO_4^-). Higher current densities were not studied in this work since they imply in elevated system temperatures and higher ozone decomposition. In addition, the envisioned application of this system is the degradation of pollutants in groundwater. The groundwater movement is often very slow and, therefore, the pollutant residence time in the electrolytic barrier is very high. Thus, it may be not necessary to apply higher current values aiming at producing elevated quantities of ozone.

The variation of dissolved ozone concentration with electrolysis time is presented in Fig. 4. It may be noticed that the stable dissolved ozone concentration was attained after approximately 50 min, when the current densities were 1.0 and 1.5 kA m^{-2}. For 0.5 kA m^{-2} this concentration was reached after 60 min. It may be also observed that the stable ozone concentration increased with increasing current density. The ozone concentrations for 1.0 kA m^{-2} and 1.5 kA m^{-2} were similar, but the generation rate for 1.5 kA m^{-2} was twice the rate for 1.0 kA m^{-2}.

3.2. Batch degradation of atrazine

The results of the batch degradation of atrazine for current densities of 0.5, 1.0 and 1.5 kA m^{-2} are presented in Fig. 5 and indicate that the atrazine degradation rate increased with current density.

At low pHs, the degradation of atrazine occurs directly by oxidation with molecular ozone (O_3). The direct ozonation of atrazine hardly causes its complete degradation [12]. On the other hand, in basic conditions the oxidation effectiveness of the ozonation process is significantly enhanced. This can be attributed to the predominance of the indirect degradation mechanism that includes the generation of hydroxyl radicals (•OH) due to the ozone decomposition in aqueous solution catalyzed by the hydroxyl ion (OH^-), according to the reaction $O_3 + H_2O \rightarrow {}^{\bullet}OH + O_2 + HO_2$. At pH 7, the decomposition of ozone occurs with the formation of •OH and the atrazine is degraded both by the direct reaction with O_3 and by the indirect reaction with •OH. The Ti/β-PbO_2 electrode is an efficient generator of •OH because oxides in which the oxidation state of the cation is the highest possible may accumulate hydroxyl radical on their surfaces [13]. The production of the oxidant species •OH and O_3 also increases with augmenting current density. In addition, the electrochemical reduction of triazines in neutral aqueous solutions is practically not observed [14,15]. The neutral pH was chosen with the purpose of simulating groundwater conditions.

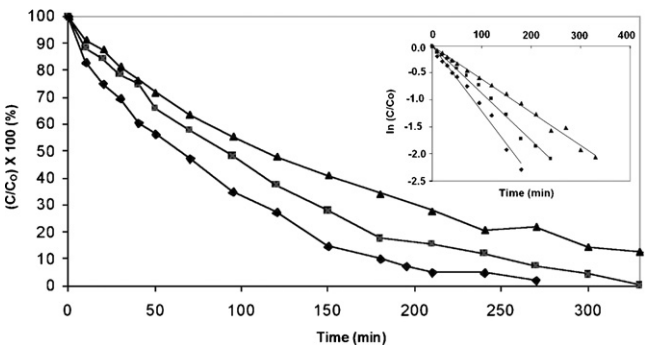

Fig. 5. Batch degradation of atrazine (▲) 0.5 kA m^{-2}; (■) 1.0 kA m^{-2} (♦) 1.5 kA m^{-2}. Inset: Corresponding kinetic analysis assuming a pseudo first-order reaction for atrazine decay.

The degradation data was adequately fitted (correlation coefficients above 0.99) by the pseudo first-order kinetic Eq. (3), as observed in Fig. 5.

$$\ln\left(\frac{C}{C_0}\right) = -kt \tag{3}$$

where C is the atrazine concentration, C_0 is the initial atrazine concentration, k is the pseudo first-order rate constant and t is the reaction time.

The values of the rate constants for the pseudo first-order equation are 6.2×10^{-3}, 8.8×10^{-3}, and 1.2×10^{-2} min^{-1} for 0.5, 1.0, and 1.5 kA m^{-2}, respectively.

It was observed that in the final stages of degradation, when the atrazine concentration was less than approximately 10% of its initial value, the reaction kinetics departed from the pseudo first-order equation. A similar behavior was observed by Murugananthan et al. [16] when studying the electrochemical degradation of 17β-estradiol and was explained by the fact that for higher concentrations the degradation rate depended basically on the current density. When the concentration diminished to a certain level, the rate turned out to be influenced by atrazine diffusion from the bulk of the solution to the electrode surface. Therefore, it may be concluded that the control of the atrazine oxidation rate was electrochemical up to approximately 90% of degradation and by mass transfer thereafter.

Fig. 6 summarizes a series of HPLC chromatograms of solution samples taken at different times, when the current density was of 1.5 kA m^{-2}. It can be observed that the atrazine peak gradually disappeared while other products with lower molecular weights and greater polarities were formed. With passing time, these composites were also transformed according to the reduction in the areas of the peaks with retention times 5.011 min, 5.727 min and 6.324 min. On the other hand, the areas of the peaks with retention times 3.776 min and 4.064 increased during the course of the experiments. As shown in Fig. 6, only the peaks 1 and 2 emerged after 360 min. For the other current densities (0.5 and 1.0 kA m^{-2}) the same atrazine decomposition pattern was verified. Hence, a dependence of the atrazine degradation mechanism (by-products formation) on ozone concentration was not detected.

According to the literature [17], the degradation of atrazine by advanced oxidative processes that do not use UV radiation is mainly accomplished by the dealkylation of the atrazine molecule and a posterior slow dechlorination. The alkyl group that is firstly removed from the atrazine molecule when it reacts with ozone is the ethyl group. This explains the greater presence of DEA than that of DIA in the chromatograms.

The retention times for the main peaks of the chromatogram presented in Fig. 6, for 95 min of degradation, are given in Table 3. In addition to the peak corresponding to atrazine five other peaks were detected.

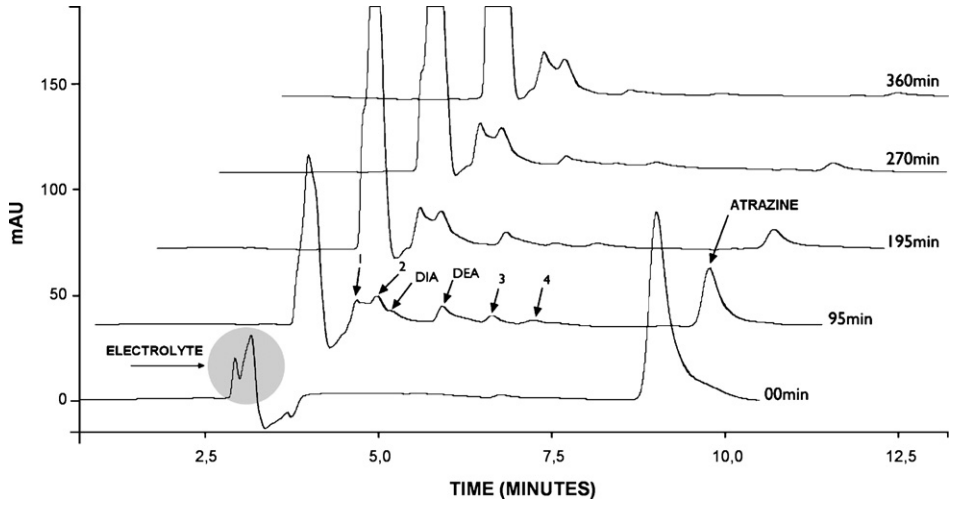

Fig. 6. HPLC chromatograms for atrazine degradation with O_3/•OH (1.5 kA m^{-2}; pH 7; 0.1 M phosphate buffer solution +1 mg L^{-1} of atrazine).

It is very likely that one of the final products obtained after 360 min of reaction is the 2-chloro-4,6-diamino-s-atrazine also known as desethyldesisopropyl-atrazine. The dechlorination of desethyldesisopropylatrazine brings about the formation of 2-hydroxy-4,6-diamino-s-atrazine (ammeline) which may be another end product of degradation. Peak 2 in Fig. 6 (retention time 4.064 min) should correspond to desethyldesisopropylatrazine since it emerged before peak 1 (retention time 3.776 min). Therefore, peak 1 should correspond to ammeline. This behavior was also observed during the degradation of atrazine with the Fenton reagent [18].

Among the observed peaks, the identification of those corresponding to DEA and DIA was possible. However, only the quantification of DEA with time was achieved, since the peak of DIA and peak 2 were not well separated. In any event, the concentration of the chemical corresponding to peak 2 seems to be low during the degradation runs. The variation of DEA concentration with time is depicted in Fig. 7. DEA concentration initially increased up to about 0.085 mg L^{-1}, which is almost 10% of the initial atrazine concentration. After 2 h the concentration of this by-product started to decrease, probably as a consequence of subsequent degradation.

Regarding the toxicity, Stratton [19] determined the toxic effects of atrazine and four of its degradation products. Atrazine was significantly more toxic than the by-products towards the tested criteria. Nélieu et al. [20] Point out that the hydroxytriazines as the ammeline are less toxic than the chlorotriazines as the atrazine.

3.3. Continuous degradation of atrazine

3.3.1. Mass transfer experiments

Fig. 8 depicts the results of the mass transfer tests as well as the curve fitting for the applied one-dimensional advection–dispersion equation. The shape of the curve corresponds to homogeneous column packing where preferential paths for mass flow are not formed. A satisfactory correlation between the experimental data and the fitted curve is observed, indicating that Eq. (2) can be successfully applied to model the experiments.

Table 4 presents the parameters obtained for the porous bed. These parameters were obtained without passing current through the electrodes. When current is applied and gases evolve, the dis-

Table 3
Retention times of the main peaks of the chromatogram presented in Fig. 6 for 95 min of degradation.

Peak	Retention time (min)
1	3.776
2	4.064
DIA	4.318
DEA	5.011
3	5.727
4	6.324
Atrazine	9.00

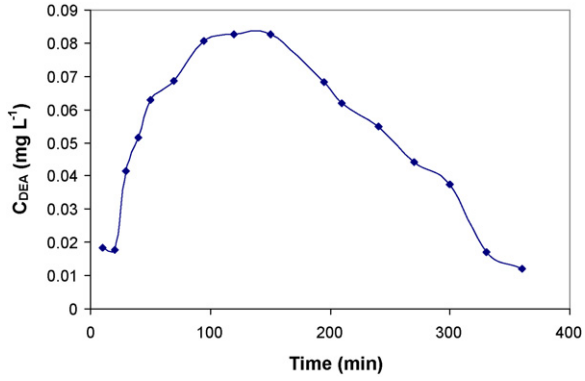

Fig. 7. Variation of DEA concentration with time (1.5 kA m^{-2}; pH 7; 0.1 M buffer phosphate solution +1 mg L^{-1} of atrazine).

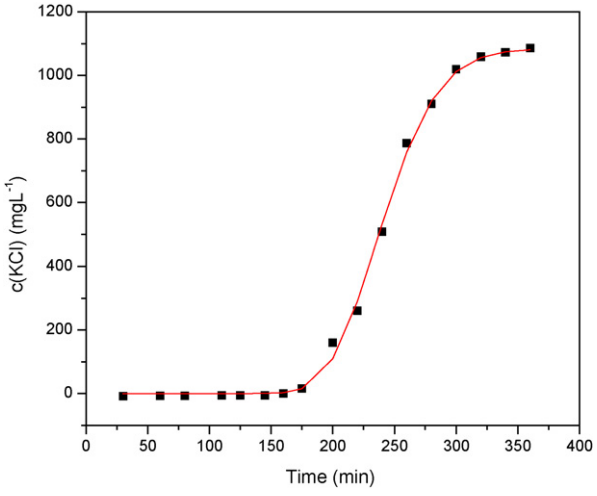

Fig. 8. Mass transfer experiment and curve fitting of data.

Table 4
Porous bed parameters obtained from mass transfer experiments and a one-dimensional advection–dispersion equation.

Dispersion coefficient ($cm^2\ min^{-1}$)	0.03
Interstitial velocity ($cm\ min^{-1}$)	0.11
Dispersivity (cm)	0.28
Porosity (–)	0.39
Mean residence time (min)	240

persion coefficient and the percolation velocity of the solution through the pores are affected. The change in the dispersion coefficient depends on factors such as the applied current intensity and the volumetric flow. Under intermediate flow rates (about 0.5 mL min^{-1}), an increase in the electric current yields an increase in the dispersion coefficient. Conversely, at higher flow rates (about 1.5 mL min^{-1}) an increment in electric current causes a decrease in the dispersion coefficient [21].

3.3.2. Atrazine degradation in column experiments

Atrazine degradation tests were conducted in the column under continuous regime with the purpose of determining whether the *in situ* electrochemical production of the oxidants $^{\bullet}OH/O_3$ is effective at reducing the atrazine concentration in the transported flux across the porous medium.

The batch degradation results were taken as a basis to set values for the current used in the continuous tests. In the batch runs, when the applied current density was 1.0 kA m^{-2} with a total charge amount of 32,400 C passing through the electrodes, the normalized charge with respect to the solution volume was 81 C mL^{-1}. In the continuous runs, for a volumetric flow rate of 0.5 mL min^{-1}, 2 min are necessary to flow 1 mL of solution through the column. Hence, to obtain the same value of charge density, 81 C should pass through the electrodes in 2 min, which corresponds to 0.67 A. Following the same procedure when the applied current density was 0.5 kA m^{-2} in the batch experiments, a current of 0.39 A was achieved. Therefore, 0.6 A and 0.4 A were the values of current utilized in the continuous tests.

Fig. 9 exhibits the concentration profiles in the column after passing electric current through the electrodes during 8 h. The experiments were carried out at 0.4 A, 0.6 A, and without current (control test). It is verified that the atrazine concentration diminishes along the column as a function of the applied current. The concentration at a location 6.5 cm downstream of the electrodes is significantly smaller than at the same place upstream of the electrodes, suggesting that the degradation occurred predominantly on or close to the electrode surface.

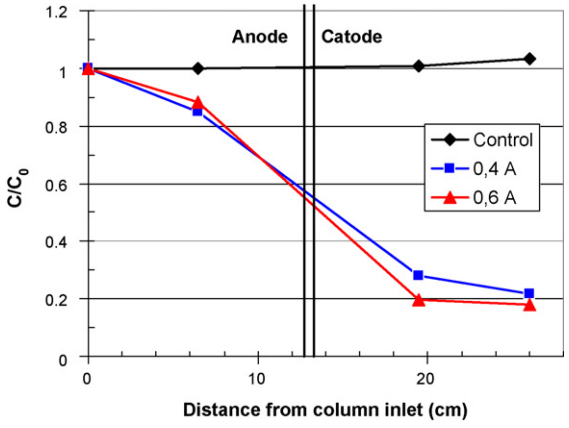

Fig. 9. Normalized concentration profile of atrazine with respect to the inlet concentration after 8 h of degradation for different positions in the column.

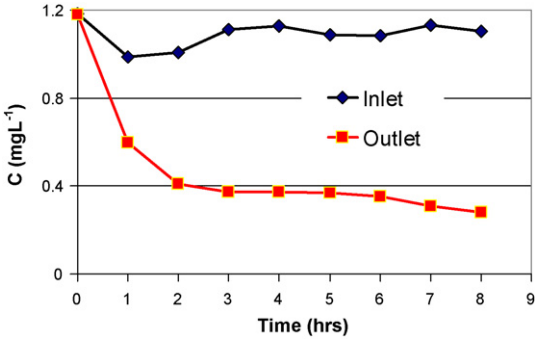

Fig. 10. Inlet and outlet atrazine concentrations as a function of time for 0.4 A.

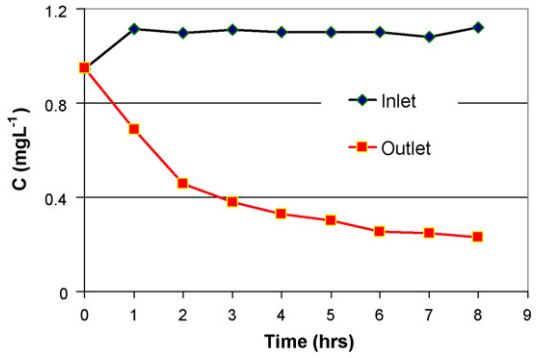

Fig. 11. Inlet and outlet atrazine concentrations as a function of time for 0.6 A.

The variation of the inlet and outlet atrazine concentrations with degradation time for 0.4 A and 0.6 A are shown in Figs. 10 and 11, respectively. The inlet concentrations varied in the range 1.0–1.2 mg L^{-1} and the outlet concentrations decreased continuously with time. The fractional oxidation of atrazine was calculated by the ratio of the difference between the inlet and outlet atrazine concentrations to the inlet atrazine concentration. Fractional oxidations of 80% for 0.6 A and 75% for 0.4 A were determined.

The above results clearly demonstrates the potential applicability of the continuous system studied for *in situ* atrazine degradation in underground waters, and provides a basis for the future development of this technology.

4. Conclusions

The rate of ozone generation by water electrolysis using a Ti/β-PbO_2 electrode as anode increased with increasing current density. The maximum rate was approximately 40 mg h^{-1} for a current density of 1.5 kA m^{-2} and the electrochemical efficiency was around 6%.

The ozone saturation concentration increased with increasing current density. For 1.5 kA m^{-2} the concentration was 1.6 mg L^{-1}. The stable dissolved ozone concentration was attained after approximately 50 min when the current densities were 1.0 and 1.5 kA m^{-2}. For 0.5 kA m^{-2} the dissolved ozone concentration was reached after 60 min.

The atrazine degradation rate increased with increasing current density. The degradation data followed a pseudo first-order kinetic equation. The values of the rate constants were 6.2×10^{-3}, 8.8×10^{-3}, and 1.21×10^{-2} min^{-1} for 0.5, 1.0, and 1.5 kA m^{-2}, respectively.

The degradation took place by the combined oxidation with O_3 and $^{\bullet}OH$ generated at the Ti/PbO_2 anode surface and by ozone decomposition. The rate was electrochemically controlled up to around 90% of degradation and by mass transfer thereafter. The

degradation mechanism was comprised mainly by dealkylation followed by a slow dechlorination of the atrazine molecule. The atrazine peak gradually disappeared while other products with lower molecular weights and greater polarities were formed. With passing time, these chemicals were also transformed.

Fractional oxidations of atrazine of 75% and 80% were accomplished in a column containing a porous media for 0.4 A and 0.6 A, respectively. The potential applicability of this system for *in situ* degradation of atrazine in underground waters was demonstrated.

References

[1] U. Dörfler, E.A. Feicht, I. Scheunert, S-Triazine residues in groundwater, Chemosphere 35 (1997) 99–106.
[2] M. Graymore, F. Stagnitti, G. Allinson, Impacts of atrazine in aquatic ecosystems, Environ. Int. 26 (2001) 483–495.
[3] A.H. Wani, B.R. O'Neal, D.M. Gilbert, D.B. Gent, J.L. Davis, Electrolytic transformation of ordinance related compounds in groundwater: laboratory mass balance studies, Chemosphere 62 (2006) 689–698.
[4] A.G. Vlyssides, M. Loizidou, P.K. Karlis, A.A. Zorpas, D. Papaioannou, Electrochemical oxidation of a textile dye waste water using a Pt/Ti electrode, J. Hazard. Mater. 70 (1999) 41–52.
[5] A.G. Vlyssides, D. Arapoglou, S. Mai, E.M. Barampouti, Electrochemical detoxification of four phosphorothioate obsolete pesticides stocks, Chemosphere 58 (2005) 439–447.
[6] G. Gordon, K. Rakness, D. Vomehm, D. Wood, Limitations of the iodometric determination of ozone, J. Am. Water Works Assoc. 81 (1989) 72–76.
[7] H. Bader, J. Hoigné, Determination of ozone in water by the indigo method, Water Res. 15 (1981) 449–456.
[8] C.W. Fetter, Contaminant Hydrology, Macmillan Publishing Company, New York, 1993.
[9] P.C. Foller, C.W. Tobias, The anodic evolution of ozone, J. Electrochem. Soc. 129 (1982) 506–515.
[10] L.M. da Silva, L.A. de Farias, J.F.C. Boodts, Electrochemical ozone production: influence of the supporting electrolyte on kinetics and current efficiency, Electrochim. Acta 48 (2002) 699–709.
[11] J.E. Graves, D. Pletcher, R.L. Clarke, F.C. Walsh, The electrochemistry of Magnéli phase titanium oxide ceramic electrodes Part II: Ozone generation at Ebonex and Ebonex/lead dioxide anodes, J. Appl. Electrochem. 22 (1992) 200–203.
[12] L. Claudia, Bianchi, Carlo Pirola, Vittorio Ragaini, Elena Selli, Mechanism and efficiency of atrazine degradation under combined oxidation processes, Appl. Catal. B 64 (2006) 131–138.
[13] C. Comninellis, Electrocatalysis in the electrochemical conversion/combustion of organic pollutants for waste water treatment, Electrochim. Acta 39 (1994) 1857–1862.
[14] L.M. Ignjatovic, D.A. Markovic, D.S. Veselinovic, B.R. Besic, Polarographic-behavior and determination of some s-triazine herbicides, Electroanalysis 5 (1993) 529–533.
[15] L. Pospíšil, R. Trsková, R. Fuoco, M.P. Colombini, Electrochemistry of s-triazine herbicides: Reduction of atrazine and terbutylazine in aqueous solutions, J. Electroanal. Chem. 395 (1995) 189–193.
[16] M. Murugananthan, S. Yoshihara, T. Rakuma, N. Uehara, T. Shirakashi, Electrochemical degradation of 17β-estradiol (E2) at boron-doped diamond (Si/BDD) thin film electrode, Electrochim. Acta 52 (2007) 3242–3249.
[17] C.L. Bianchi, C. Pirola, V. Ragaini, E. Selly, Mechanism and efficiency of atrazine degradation under combined oxidation processes, Appl. Catal. B 64 (2006) 131–138.
[18] A.D. Saltamira, A.T. Lemley, Atrazine degradation by anodic Fenton treatment, Water Res. 36 (2002) 5113–5119.
[19] G.W. Stratton, Effects of the herbicide atrazine and its degradation products, alone and in combination, on phototrophic microorganisms, Arch. Environ. Contam. Toxicol. 13 (1984) 35–42.
[20] S. Nélieu, L. Kerhoas, J. Einhorn, Degradation of atrazine into ammeline by combined ozone/hydrogen peroxide treatment in water, Environ. Sci. Technol. 34 (2000) 430–437.
[21] M.A. Petersen, Characterizing reaction and transport processes in an electrolytic reactor for *in situ* groundwater treatment, PhD Theses, Department of Chemical & Biological Engineering, Colorado State University, Fort Collins, 2007, p. 177.